A Comparative Study of Stress-Induced Crystallization of Guayule, Hevea, and Synthetic Polyisoprenes

YASUSHI SHIMOMURA,* JAMES L. WHITE, and JOSEPH E. SPRUIELL, *Polymer Engineering, University of Tennessee, Knoxville, Tennessee 37996*

Synopsis

A comparative study of the stress induced crystallization of natural (Hevea, Guayule) and synthetic high cis-1,4-polyisoprenes at room temperature is presented. Hevea and Guayule are both found using WAXS to crystallize into the unit cell of Morss and Bunn previously described for Hevea. DSC studies of polyisoprenes held at −25°C indicate that Hevea and Guayule crystallize more rapidly than synthetics. Studies of relative birefringence and stress decay following uniaxial extension confirm this. Under conditions of comparison at the same stress, raw Hevea crystallizes more rapidly than extracted Hevea, Guayule, and the other polyisoprenes.

INTRODUCTION

Cis-1,4-polyisoprenes play an important role in technology, especially as a major component of tires. For many years, the only generally available cis-1,4-polyisoprene elastomer was the polymer naturally occurring in the latex of the *Hevea brasiliensis* tree.[1,2] It has, however, long been realized that this material is only one of many cis-1,4-polyisoprenes occurring in plants,[3–6] though most of these are of low molecular weight. Certainly the most important of these is the high molecular weight cis-1,4-polyisoprene deriving from the *Guayule* bush. While this material has a long history,[7,8] it has only been in recent years that a high quality relatively resin-free grade has become available in sizeable quantities through the efforts of the Mexican government.[9,10] In addition, various synthetic polyisoprenes, many of them with high cis-1,4-microstructures, have been synthesized through the years.[11–14] At least two synthetic polyisoprenes are commercially available.

One of the most striking characteristics of the Hevea cis-1,4-polyisoprene is its ready ability to crystalize on stretching.[15–21] It is known that synthetic high cis-1,4-polyisoprenes may also crystallize upon stretching.[12,13,22] There has, however, been little direct comparison of this tendency among different polyisoprenes in the literatuare. Researchers on synthetic polyisoprenes generally remark that crystallization occurs more slowly than for Hevea. Preliminary studies for Guayule have indicated that it also crystallizes more slowly than Hevea.[23] The differences in rates of crystallization have been hypothesized to be due to varying levels of cis-1,4 content or to impurities. Evidence for the latter has come from studies on raw and extracted Hevea, which indicates the former crystallizes more readily.[24]

---

* Present address: Ube Industries, Hirakata Plastics Laboratory, Hirakata, Osaka, Japan.

TABLE I
Unit Cells Determined for Natural Rubber

Author	Unit cell dimensions (Å)			Angles of unit cell			Remarks
	a	b	c	α	β	γ	
Mark and von Susich[25]	12.3	8.3	8.1	90°	90°	90°	Orthorhombic
Morss[26] I	26.3	8.9	8.15	90°	90°	109.5°	Monoclinic
II	12.4	8.9	8.15	90°	90°	90°	Orthorhombic
Bunn[9]	12.46	8.89	8.10	90°	92°	90°	Monoclinic

In this paper, we present a basic comparative study of stress-induced crystallization of high cis-1,4-polyisoprenes. We investigate both naturally occurring and synthetic polyisoprenes, including *Hevea* and *Guayule*. Specifically, we compare (i) wide angle X-ray diffraction patterns of stretched polyisoprene samples, (ii) rates of stress-induced crystallization as determined by the relative rates of birefringence and stress relaxation, (iii) uniaxial stress–strain measurement, and (iv) differential scanning calorimetric responses of amorphous and crystalline elastomers.

BACKGROUND

Crystal Structure

There have been numerous studies of the crystal structure of Hevea rubber[25–28] using wide angle X-ray diffraction (WAXS). Layer line spacings have indicated a repeat distance of 8.1 Å. Stretched highly oriented samples possess two strong equatorial reflections at 6.2 Å and 4.1 Å.

The detailed WAXS pattern results have been interpreted in terms of both orthorhombic and monoclinic unit cells as summarized in Table I. In terms of the unit cells of Morss (II)[26] and Bunn,[27] the 6.2 Å reflection corresponds to the 200 reflection and the 4.1 Å reflection to the 120.

A planar zigzag cis-1,4-polyisoprene unit may be shown from molecular models to have a polymer chain axis repeat distance of 9.2 Å, which differs significantly from the 8.1 Å value found. This must indicate rotations about a single bond in the backbone as noted by Morss,[26] Bunn,[27] and Nyburg.[28]

Birefringence in Stretched Elastomers and Crystallization

The birefringence of stretched elastomers corresponds to molecular orientation. As first shown by Hermans and his co-workers,[29] the birefringence of a uniaxially oriented homogenous material may be expressed as

$$\Delta n = f \Delta^0 \tag{1}$$

with

$$f = \frac{1}{2}[3\overline{\cos^2\phi - 1}] \tag{2}$$

where Δn is the observed birefringence, Δ^0 is the maximum on intrinsic birefringence, and f is the Hermans orientation factor. In a partially crystalline polymer, Δn may be expressed as the sum of birefringences of two different phases, and a form birefringence[30,31]:

TABLE II
Polyisoprene Samples Used in This Study

Polymer	Supplier	% cis-1,4	M_n	M_w/M_n
Hevea	BFGoodrich	100	7.06	3.24
Guayule	CIQA	100	5.92	2.19
2200	Goodyear Natsyn	97	5.67	3.08
305	Shell Cariflex	93	6.10	2.73

$$\Delta n = \phi_c f_c \Delta_c^0 + (1 - \phi) f_a \Delta_a^0 + \Delta n_{\text{form}} \qquad (3)$$

Here ϕ_c is the volume faction crystallinity, Δn_{form} is the form birefringence,[32] and the subscripts c and a correspond to the crystalline and amorphous phases.

It has been well established that various elastomers and molten plastics[17,32–37] including Hevea[17,32,34] obey the Rheooptical Law, which may be stated as

$$n_1 - n_2 = C(\sigma_1 - \sigma_2) \qquad (4a)$$

or for uniaxially stretched samples

$$\Delta n = C\sigma \qquad (4b)$$

where σ represents stress, C the stress optical constant, and the subscript i refers to the principal direction. From eq. (1) this implies that, in uniaxial extension, the Hermans orientation factor is related to the stress in amorphous polymers through

$$f_a = (C/\Delta_a^0)\sigma \qquad (5)$$

When crystallization occurs in uniaxial stretching, there is generally a sudden rise in birefringence.[16,17,38,39] This would seem to correspond to the much higher level of orientation in the crystalline as opposed to the amorphous regions. Taylor and Darin[40] have proposed that the level of crystallinity ϕ_c may be determined experimentally by solving Eq. (3) to give

$$\phi c = \frac{\Delta n - f_a \Delta_a^0}{f_c \Delta_c^0 - f_a \Delta_a^0} \qquad (6)$$

**On–Line Measurement of Birefringence in
Crystallizing Samples**
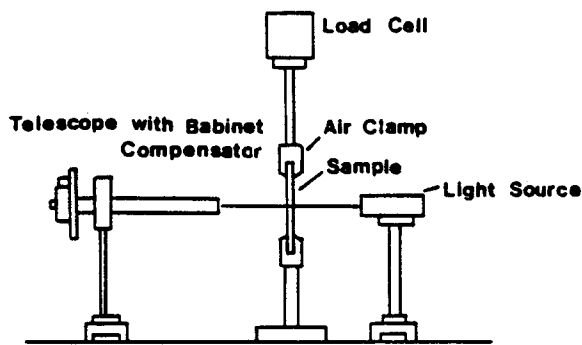
Stretching Rate: 2500 %/min.

Temperature: 24-26 °C

Fig. 1. Apparatus for on-line birefringence of stretched samples.

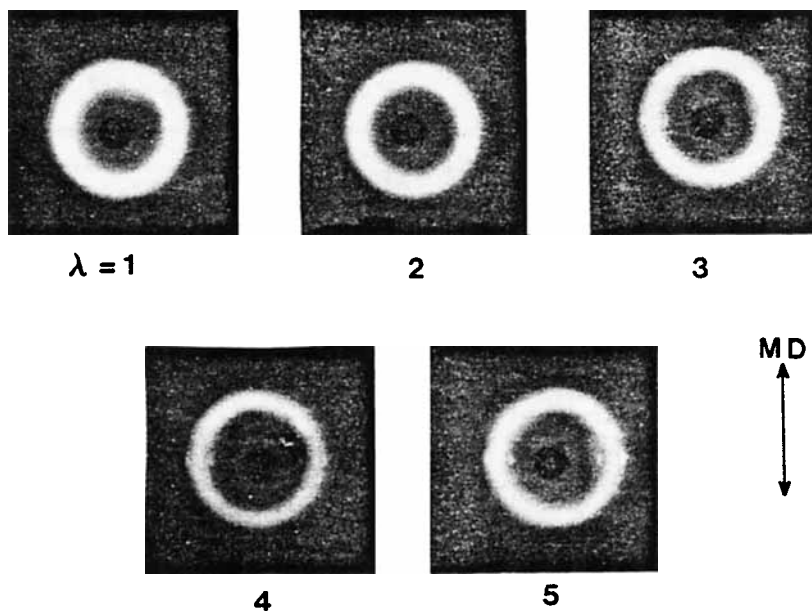**Hevea (Raw) , Exposed for 3 hrs after stretching**

Fig. 2. WAXS pattern for stretched and crystallized Hevea.

where Δn_{form} is neglected.

The value of f_a at low levels of crystallization was taken to be given by eq. (5). This leads to

$$\phi_c = (\Delta n - C\sigma)/(f_c \Delta_c^0 - C\sigma) \tag{7}$$

Equation (7) was used by Taylor and Darin[40] to investigate crystallization of polybutadiene and more recently by Kraus and Gruver[41] for polypentenamer, and by Hashiyama, Gaylord, and Stein[22] for synthetic *cis*-1,4-polyisoprene vulcanizates.

Guayule (Extracted)   I R 2200

$\lambda = 4$,   **3 hrs**
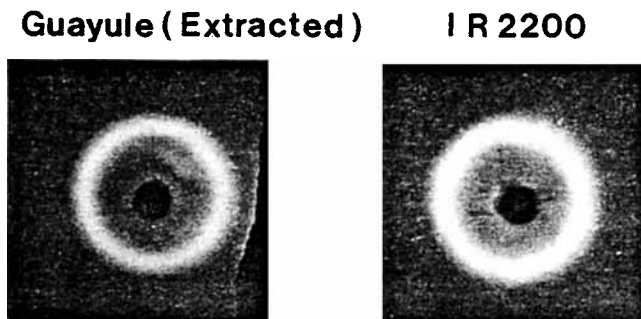
Fig. 3. WAXS pattern for stretched, cooled (−3°C), crystallized Guayule, and 2200.

In order to apply eq. (7) it is necessary to know f_c, C, and Δ_c^0. The value of f_c can be surmised from WAXS and C from birefringence–stress data on the amorphous elastomer. Various values of Δ^0 have been quoted in the literature. Treloar[17] surmised a value of 0.28 for Δ_a^0 of Hevea. Hashiyama et al.[42] calculated a value of 0.13, presuming tensor additivity of bond polarizabilities.

EXPERIMENTAL

Materials

Four high *cis*-1,4 polyisoprenes were used in this study. These include samples of Hevea and Guayule natural rubber and Goodyear Natsyn® 2200 and Shell Cariflex® 305 synthetic high *cis*-1,4 polyisoprenes. Table II summarizes microstructures and molecular weight distributions determined for these elastomers in the laboratories of CIQA.

Samples of the Hevea and Guayule were also extracted by acetone with a Soxhlet extractor for 3 days.

Preparation of Films

Films of the various polyisoprenes were prepared by compression molding at 110°C for 2 h.

WAXS Measurements on Films

Films were stretched in a mechanical device consisting of one fixed clamp and one clamp attached to a screw. After stretching to the desired draw ratio, the
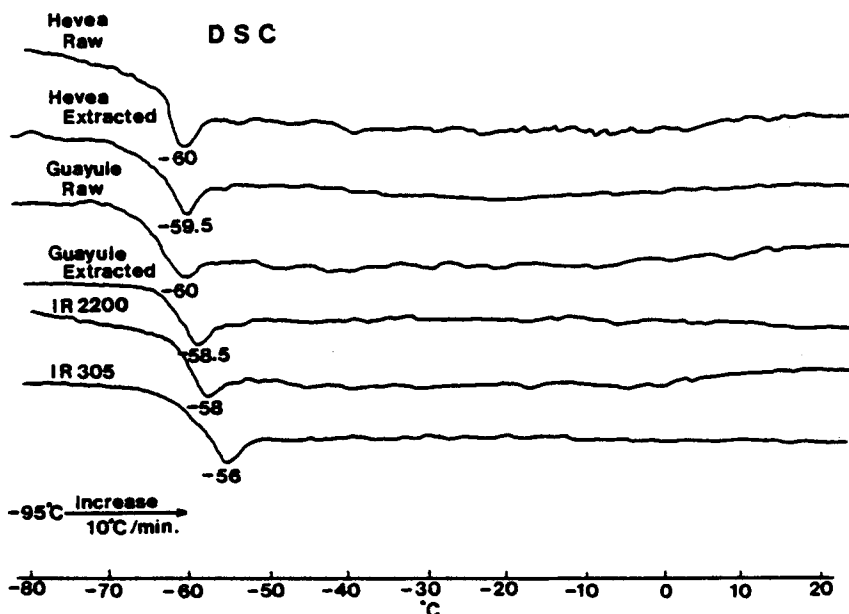

Fig. 4. DSC traces for Hevea, Guayule, 2200, and 305.

entire device could be placed in a collimated X-ray beam from a Philips X-ray generator. In this arrangement the specimen to film distance was 3.7 cm. The radiation was Ni filtered Cu Kα with wavelength 1.5418 Å.

Uniaxial Tensile Stretching

The films were stretched in an Instron tensile testing machine at room temperature at a crosshead velocity of 8.33 cm/s.
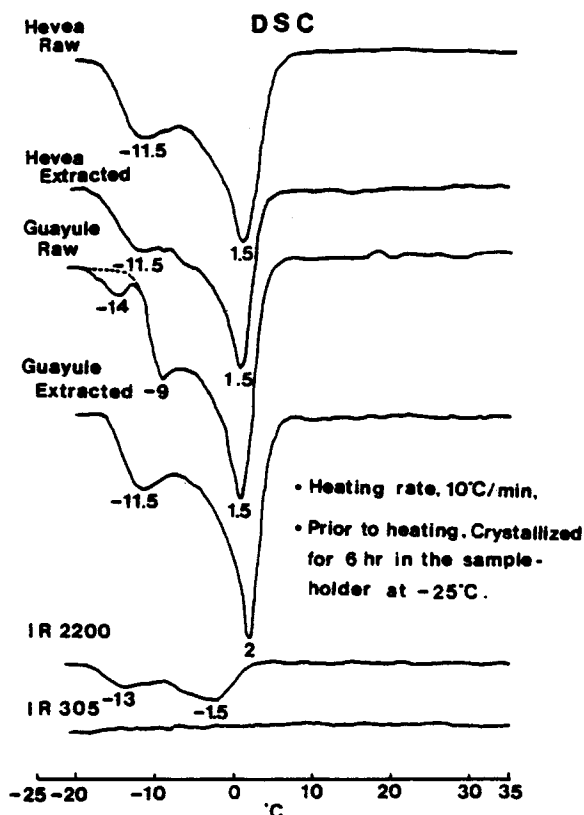

Fig. 5. DSC Traces for Hevea, Guayule, 2200, and 305 crystallized at −25°C.

TABLE III
WAXS Reflections Observed for *Cis* Polyisoprenes

WAXS reflection d-spacing		Calcd from	Indices,
Hevea	Guayule	Bunn unit cell	Bunn unit cell
(Equatorial)	(Equatorial)		
7.39	7.39	7.11	200
10.69	10.69	10.61	120
(First layer)			
9.15	—	9.13	201
12.02	—	12.03	$\bar{1}21$
			$\bar{1}21$

TABLE IV
DSC Transitions Observed for Polyisoprenes

Polymer	T_g	Melting peaks	
		Lower Temp Peak	High Temp Peak
Hevea	−60	−11.5	1.5
Guayule	−60	−9	1.5
2200	−58	−13	−1.5
305	−56	—	—
Hevea (extracted)	−59.5	−11.5	1.5
Guayule (extracted)	−58.5	−11.5	2.0

Birefringence Measurements

On-line birefringence measurements were made following the deformation process using the experimental apparatus shown in Figure 1. An optical bench containing polarizer, analyzer, and Babinet compensation were used. Both stress and birefringence decay were measured.

Differential Scanning Calorimetry

Measurements were made using a Perkin-Elmer Differential Scanning Calorimeter (DSC) Model IB. The amorphous elastomers were heated from −95°C at a rate of 10°C/min. The low temperatures were achieved using a liquid nitrogen cooling attachment.

Experiments were also carried out in which the samples were maintained for a period of 6 h at −25°C in the DSC using an ethanol/dry ice mixture for coolant. They were then heated at a rate of 10°C/min.

RESULTS

WAXS Measurements

The on-line WAXS measurements only perceived the development of crystallinity in Hevea (see Fig. 2). The existence of sharp spots rather than partial Debye rings indicates a high level of crystalline orientation.

It was possible to obtain WAXS patterns for Guayule and the 2200 by taking samples stretched and slightly crystallized and reducing their temperature to −3°C. The WAXS patterns are shown in Figure 3. The existence in both cases of sharp spots again also indicates a high level of crystalline orientation.

The observed d-spacings for Hevea and Guayule are summarized in Table III. These correspond to the principal reflections computed from Morss' and Bunn's unit cells of Table I. The comparison with d-spacings computed from Bunn's unit cell are shown in Table III. All three cis-1,4-polyisoprenes seem to have the same unit cell.

Differential Scanning Calorimetry (DSC)

DSC traces for the amorphous polymers studied at a heating rate of 10°C/min are shown in Figure 4. All of the polymers show glass transition temperatures. These are summarized in Table IV.

Each of the polyisoprenes was held in the calorimeter at −25°C for a period of 6 h during which crystallization proceeded. Following this treatment, the elastomer was heated at a rate of 10°C/min. The traces are shown in Figure 5. Endotherms representing melting transitions are observed for Hevea, Guayule, and 2200 polymers. The 305 polymer did not show such an endotherm and it must be concluded that this material does not thermally crystallize within 6 h at −25°C.
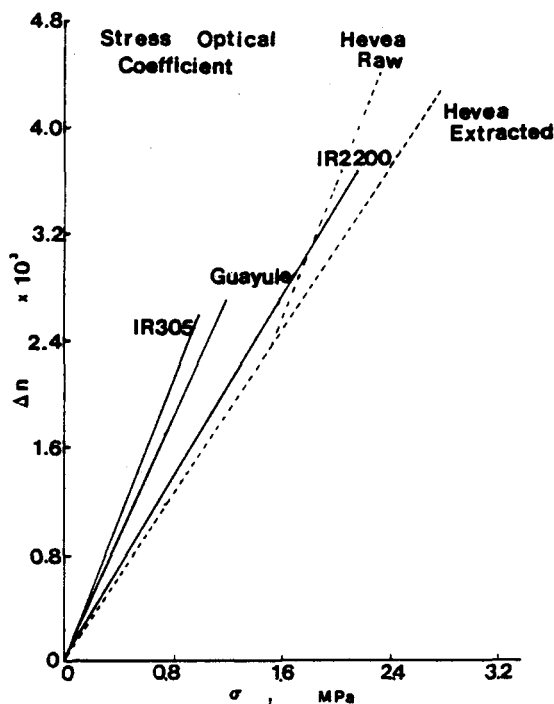
Fig. 6. Birefringence–stress data for Hevea, Guayule, 2200, and 305 at 20°C as well as for extracted Hevea and Guayule at 20°C.

TABLE V
Stress–Optical Constants

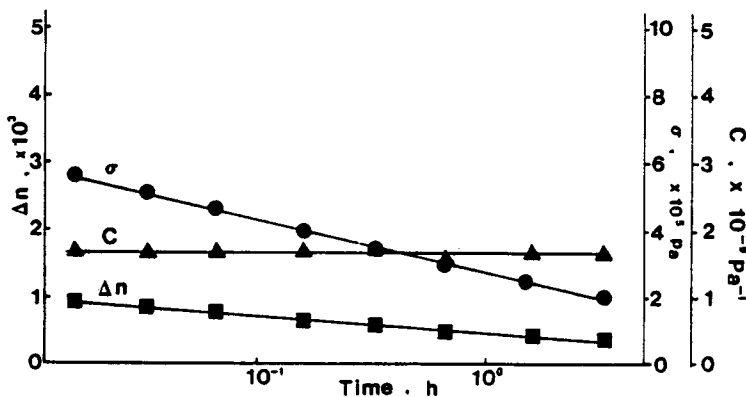| Polymer	$C \times 10^9$ (Pa^{-1})	Reference
Hevea	1.64	This paper
Guayule	2.38	This paper
2200	1.87	This paper
305	2.64	This paper
Hevea (extracted)	1.64	This paper
Guayule (extracted)	2.38	This paper
Hevea	2.33	Treloar[17]
	1.88	Saunders[34]

Fig. 7. Birefringence, stress, and stress–optical coefficients for Hevea ($\lambda = 2$) as a function of time.

Birefringence Measurements

Birefringence measurements as a function of stress are shown in Figure 6 for the Hevea, Guayule, 2200, and 305. Figure 6 also contains a similar plot for the extracted Hevea and Guayule. All of the plots are linear except the Hevea at high stresses. The stress optical constants corresponding to this are summarized in Table V.

Birefringence and stress relaxation data together with apparent stress optical constants are plotted as a function of time for Hevea in Figures 7 and 8 at different extension ratios.

Stress–Elongation Curves

Plots of true stress $\lambda F/A$, where F is force, λ is extension ratio, and A is cross-sectional area as a function of extension ratio λ, are shown in Figures 9–11. We compare Hevea and extracted Hevea in Figure 9 and Guayule and extracted
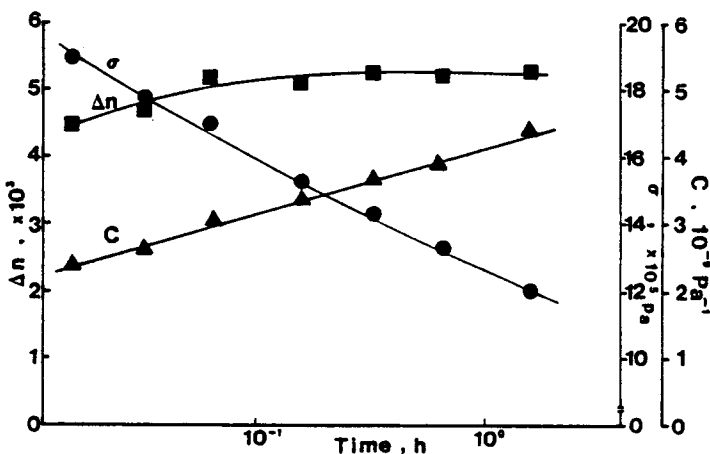
Fig. 8. Birefringence, stress, and stress–optical coefficients for Hevea ($\lambda = 4$) as a function of time.
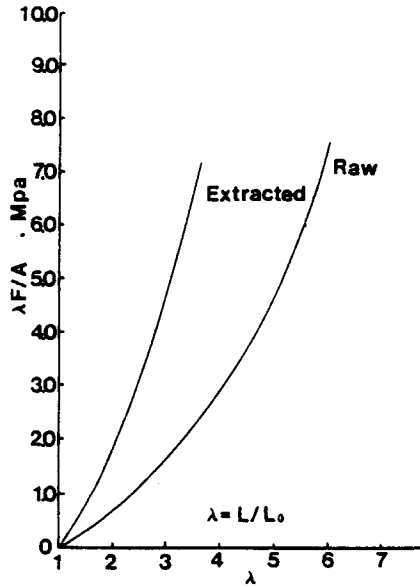
Fig. 9. True stress ($\lambda F/A$) as a function of elongation λ for Hevea and extracted Hevea.

Gauyule in Figure 10. In each case, extraction increases the stress at a fixed extension ratio. Figure 11 compares the stress–elongation curves for the 2200 and 305 polyisoprenes.
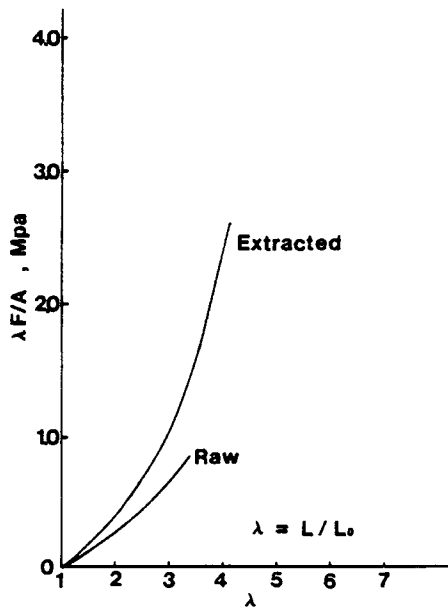

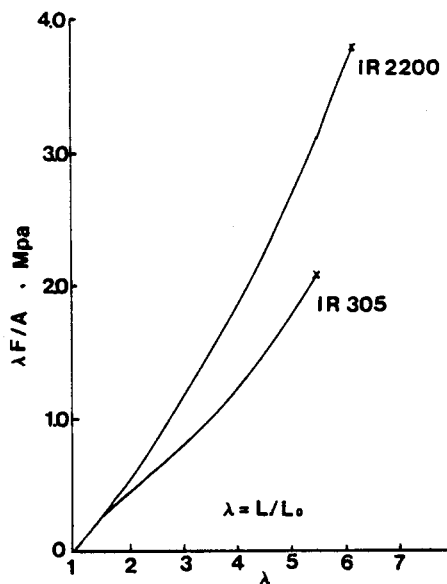Fig. 10. True stress ($\lambda F/A$) as a function of elongation λ for Guayule and extracted Guayule.

Fig. 11. True stress ($\lambda F/A$) as a function of elongation λ for 2200 and 305.

DISCUSSION

Unit Cells

The WAXS observations of this paper seem to indicate that Guayule and Hevea crystallize into the same unit cell, and this is the unit cell described by Morss,[26] Bunn,[27] and Nyburg.[28]
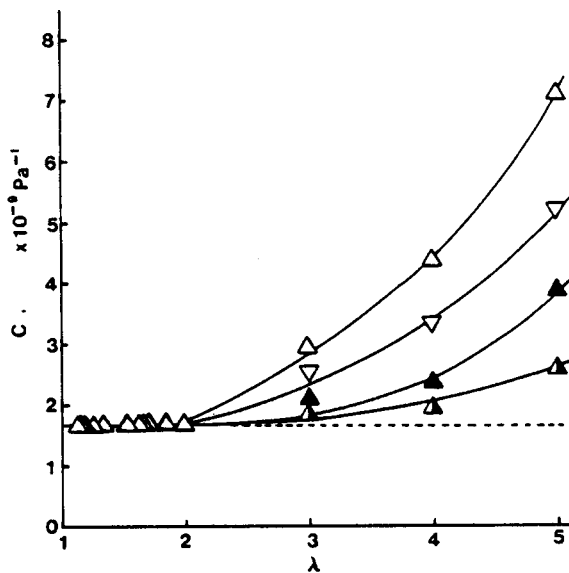
Fig. 12. Stress–optical constant as a function of extension ratio and time for Hevea. Time (h): (△) 1.6×10^{-3}; (▲) 1.6×10^{-2}; (▽) 1.6×10^{-1}; (△) 1.6×10^{0}.
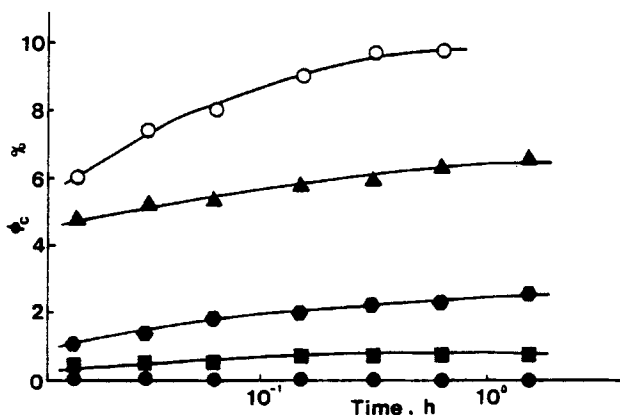
Fig. 13. Fraction of crystallinity, ϕ_c as a function of time for Hevea as a function of time at different extension ratios. λ: (●) 2.0; (□) 3.0; (●) 4.0; (▲) 5.0; (○) 6.0.

Stress–Optical Constants

Stress–optical constants computed from birefringence and stress measurements are summarized in Table V. The values range from 1.64 to 2.38 × 10⁹ Pa⁻¹. Earlier measurements of C from the literature are also listed. There is general agreement. The Hevea data and the 2200 are lower than the Guayule and the 305.

Stress-Induced Crystallization

The on-line measurements of WAXS as well as the DSC traces of Figure 5 following 6 h at −25°C indicate that Hevea crystallizes more rapidly than the other polyisoprenes of this study. The IR 2200 crystallizes less at −25°C than the Hevea and Guayule. The IR 305 crystallizes hardly at all.

At higher extension ratios, the birefringence does not decay and C increases with time. This was observed for all the polyisoprenes except the IR 305. This indicates that crystallization is occurring. Figure 12 shows the variation of C for Hevea as a function of extension ratio and time. The level of crystallinity, ϕ_c, may be computed from eq. (7). To carry out these calculations, we need to know Δ_c^0 and f_c. Following Hashiyama et al.,[22] Δ_c^0 was taken as 0.13. The WAXS patterns observed in Figure 2 indicate high levels of orientation. In particular, the 200 and 120 reflections are concentrated at the equator. This implies that the **a** and **b** crystallographic axes are perpendicular to the direction of stretch and **c** parallel to this direction. We have taken f_c to be 1.0. Figures 13–15 show calculations of ϕ_c as a function of time for raw Hevea, extracted Guayule, and IR 2200.

Detailed comparisons of the crystallization of the different elastomers are shown in Figures 16–18. A comparison at a fixed extension ratio is given in Figure 16. This indicates that at an extension ratio of 3 the extracted Hevea crystallizes more rapidly than the raw Hevea and the other polyisoprenes hardly crystallize at all. The development of crystallinity in the cis-polyisoprenes is plotted vs. stress in Figures 17 and 18. Data from different extension ratios
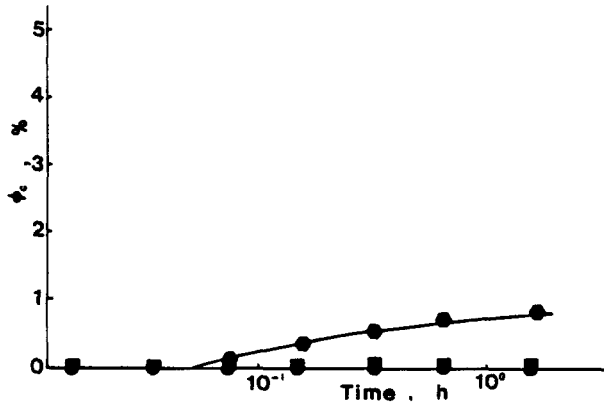
Fig. 14. Fraction of crystallinity, ϕ_c as a function of time for Guayle as a function of time at different extension ratios. λ: (●) 2; (■) 3; (●) 4.
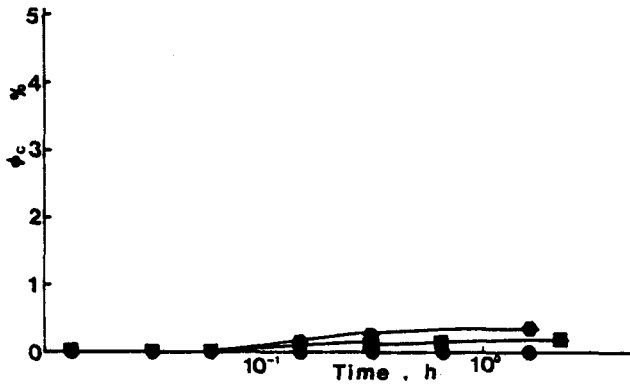

Fig. 15. Fraction of crystallinity, ϕ_c, as a function of time for IR 2200 as a function of time at different extension ratios. λ: (●) 2; (■) 3; (●) 4.
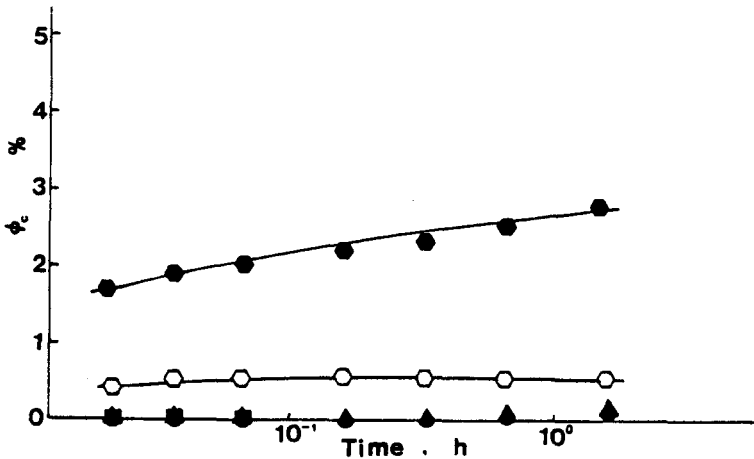

Fig. 16. Fraction of crystallinity, ϕ_c, for polyisoprenes as a function of time at fixed extension ratio $\lambda = 3$: (●) Hevea (extracted); (O) Hevea (raw); (●) Guayule (extracted); (▲) IR 2200; (■) IR 305.

obtained at the same time are included. The level of ϕ_c is seen in Figure 17 to be higher in the raw Hevea than in the extracted Hevea. Figure 18 contains a comparison of Hevea, Guayule, and the IR 2200 on this basis. Raw Hevea is found to show a more rapid development of stress. The extracted Hevea and Guayule are about the same, indicating similar behavior of natural rubber hydrocarbon from different sources.

The reason for the inverted order of the Hevea data between Figures 16 and 17–18 is due to the plasticization of the elastomer by the extract.
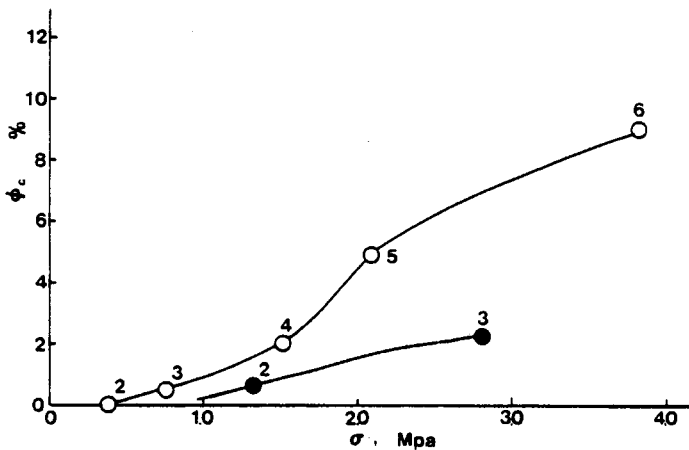

Fig. 17. Fraction of crystallinity, ϕ_c, as a function of stress at fixed time (1.6×10^{-1} h) for raw (O) and extracted (●) Hevea.
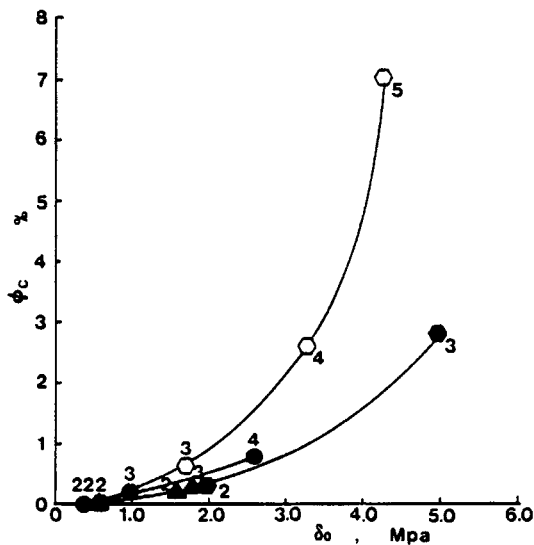

Fig. 18. Fraction of crystallinity, ϕ_c, as a function of stress at fixed time (1.6 h) for the polyisoprenes of this study: (O) Hevea (raw); (●) Hevea (extracted); (O) Guayule (extracted); (△) IR 2200.

References

1. B. L. Archer, D. Barnard, A. J. Cockbain, P. B. Dickenson, and A. I. McMullen, "Structure Composition and Biochemistry of Hevea Latex," in *The Chemistry and Physics of Rubberlike Substances*, L. Bateman, Ed., Wiley, New York, 1963.

2. P. W. Allen and G. Bloomfield, "Natural Rubber Hydrocarbon," in *The Chemistry and Physics of Rubberlike Substances*, L. Bateman, Ed., Wiley, New York, 1963.

3. F. W. Stavely, P. H. Biddison, M. J. Forster, H. G. Dawson, and J. L. Binder, *Rubber Chem. Technol.*, **34**, 423 (1961).

4. D. McIntyre, "The Chemical Structure of Guayule Rubber," in *Guayule*, CIQA, Saltillo, Mexico, 1978.

5. C. L. Swanson, R. A. Buchanan, and F. H. Otey, *J. Appl. Polym. Sci.*, **23**, 743 (1979).

6. T. Hager, A. MacArthur, D. McIntyre, and R. Seeger, *Rubber Chem. Technol.*, **52**, 693 (1979).

7. Anonymous, *Ind. Rubber World*, **109**, 475 (1944).

8. W. G. McGinnies, "Overview of Guayule Programs," in *Guayule*, CIQA, Saltillo, Mexico, 1978.

9. D. S. Winkler, H. J. Shostarez, and H. L. Stephens, "Gum Properties and Filled Stock in Guayule Rubber," in *Guayule*, CIQA, Saltillo, Mexico, 1978.

10. J. Neher, *Rubber Plast. News*, 12 (August 22, 1977).

11. W. Richardson and A. Sachen, *J. Polym. Sci.*, **14**, 353 (1953).

12. F. W. Stavely et al., *Ind. Eng. Chem.*, **48**, 778 (1956).

13. S. E. Horne et al., *Ind. Eng. Chem.*, **48**, 784 (1956).

14. F. C. Foster and J. L. Binder, *Adv. Chem.*, **19**, 26 (1957).

15. J. R. Katz, *Naturwiss.*, **13**, 410 (1925).

16. L. R. G. Treloar, *Trans. Faraday Soc.*, **37**, 84 (1941).

17. L. R. G. Treloar, *Trans. Faraday Soc.*, **43**, 284 (1947).

18. A. N. Gent, *Trans. Faraday Soc.*, **50**, 521 (1954).

19. A. V. Tobolsky and G. M. Brown, *J. Polym. Sci.*, **7**, 547 (1955).

20. E. H. Andrews and A. N. Gent, "Crystallization in Natural Rubber," in *The Chemistry and Physics of Rubberlike Substances*, L. Bateman, Ed., Wiley, New York, 1963.

21. D. J. Dunning and P. J. Pennells, *Rubber Chem. Technol.*, **40**, 1881 (1967).

22. M. Hashiyama, R. Gaylord, and R. S. Stein, *Makromol. Chem. Suppl.*, **1**, 579 (1975).

23. L. F. Ramos de Valle and M. Montelongo, *Rubber Chem. Technol.*, **51**, 863 (1978).

24. A. N. Gent, *J. Polym. Sci.*, **18**, 321 (1955).

25. H. Mark and G. von Susich, *Kolloid Z.*, **46**, 11 (1928).

26. H. A. Morss, *J. Am. Chem. Soc.*, **60**, 2371 (1938).

27. C. W. Bunn, *Proc. Roy. Soc. (Lond.), A*, **180**, 40 (1942).

28. S. C. Nyburg, *Acta Crystallog.*, **7**, 385 (1954).

29. P. H. Hermans and P. Platzek, *Kolloid Z.*, **88**, 68 (1939); J. J. Hermans, P. H. Hermans, D. Vermaas, and A. Weidinger, *Recl. Trav. Chim.*, **65**, 427 (1946).

30. P. H. Hermans, J. J. Hermans, D. Vermaas, and A. Weidinger, *J. Polym. Sci.*, **3**, 1 (1948).

31. R. S. Stein and F. H. Norris, *J. Polym. Sci.*, **21**, 381 (1956).

32. R. S. Stein and A. V. Tobolsky, *Text. Res. J.*, **18**, 302 (1948).

33. R. S. Stein, F. H. Holmes, and A. V. Tobolsky, *J. Polym. Sci.*, **14**, 443 (1954).

34. D. W. Saunders, *Trans. Faraday Soc.*, **52**, 1414 (1956).

35. J. L. S. Wales, *Rheol. Acta*, **8**, 38 (1969).

36. C. D. Han and L. H. Drexler, *J. Appl. Polym. Sci.*, **17**, 2329 (1973).

37. F. H. Gortemaker, M. G. Hansen, B. de Cindio, H. M. Laun, and H. Janeschitz-Kriegl, *Rheol. Acta*, **15**, 256 (1976).

38. K. Katayama, T. Amano, and K. Nakamura, *Kolloid Z., Polym.*, **226**, 125 (1967).

39. H. P. Nadella, H. M. Henson, J. E. Spruiell, and J. L. White, *J. Appl. Polym. Sci.*, **21**, 3003 (1977).

40. G. R. Taylor and S. R. Darin, *J. Appl. Phys.*, **20**, 1075 (1955).

41. G. Kraus and J. T. Gruver, *J. Polym. Sci., Polym. Phys. Ed.*, **10**, 7009 (1972).